PHASE SENSITIVE IMAGE RECONSTRUCTION

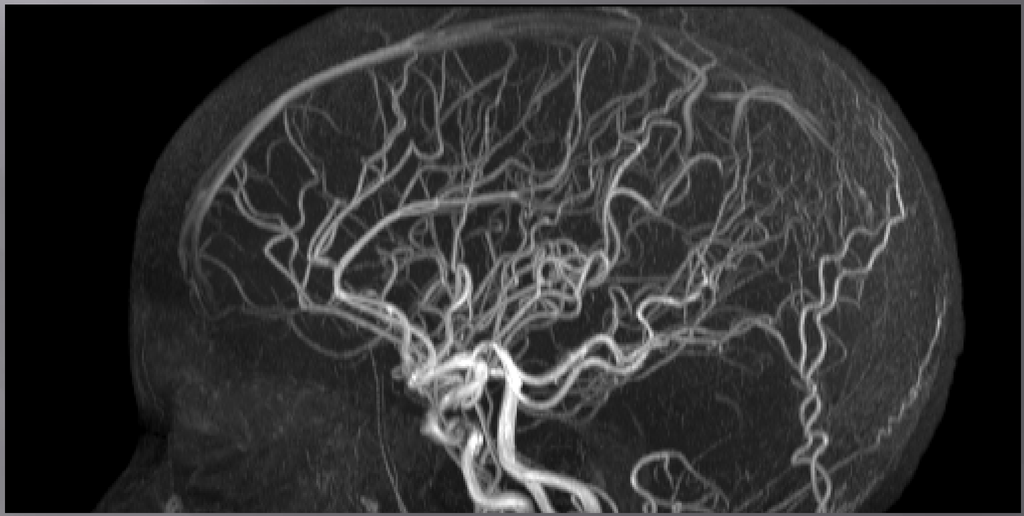

E. Mark Haacke[1], PhD and Saifeng Liu[2], PhD
[1]Director, MR Research Facility, Wayne State University
[2]Research Scientist, MRI Institute for Biomedical Research
May 31st, 2015

Conflicts of Interest

- Support from NIH grants
- Owner of MR Innovations
- Patents related to SWI and SWIM

Fundamentals

- Basics of gradient-echo signal formation
- Phase and its fundamental role in imaging
- Phase as a source of T_2* dephasing
- Methods for phase unwrapping
- Background phase/field removal

Applications

- Water/fat separation
- Flow quantification
- Temperature mapping
- Susceptibility weighted imaging (SWI)
- Quantitative susceptibility mapping (QSM)
- Measuring and visualizing conductivity

Magnetic Resonance Imaging

- Although quantum physics was needed to formulate the theoretical concepts and explain the experimental design and results in magnetic resonance, the final impact rests on the very simple relationship given by the well known Larmor equation relating the frequency of rotation or precession frequency (ω) and the local magnetic field (B) via $\omega = \gamma B$.

Visualizing Quantum Mechanics

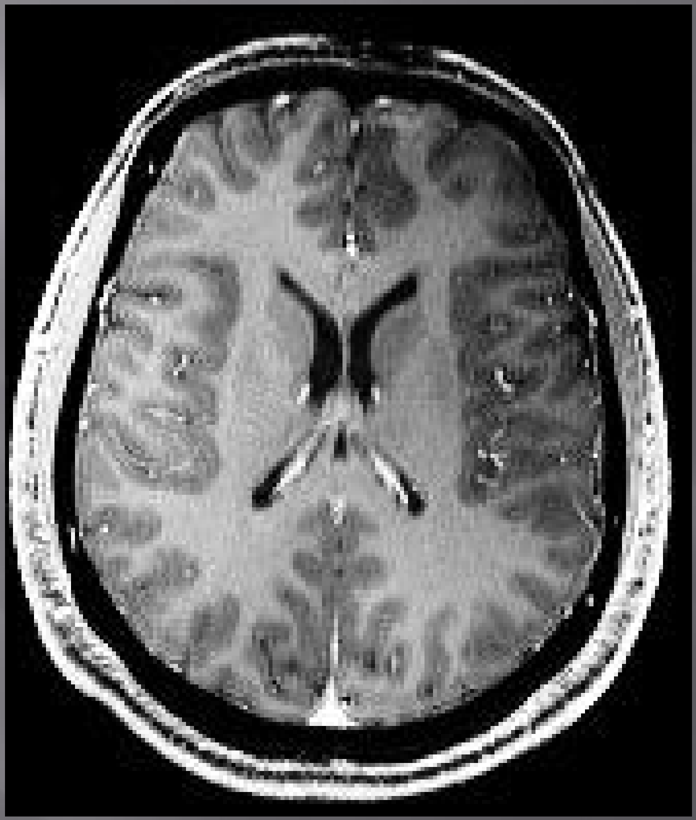

Thin slice T1 weighted post contrast 3D MRI of the brain

Basic MRI concepts

$\omega = -\gamma B$

B: the applied magnetic field

γ : the gyromagnetic ratio of the proton γ

ω: the magnetic resonance frequency

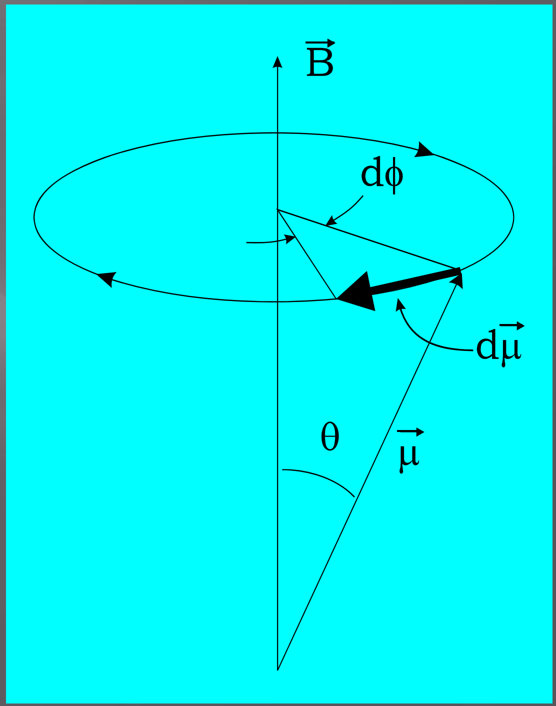

A cylindrical object in a constant magnetic field.

Its bulk magnetization lies parallel to the main field.

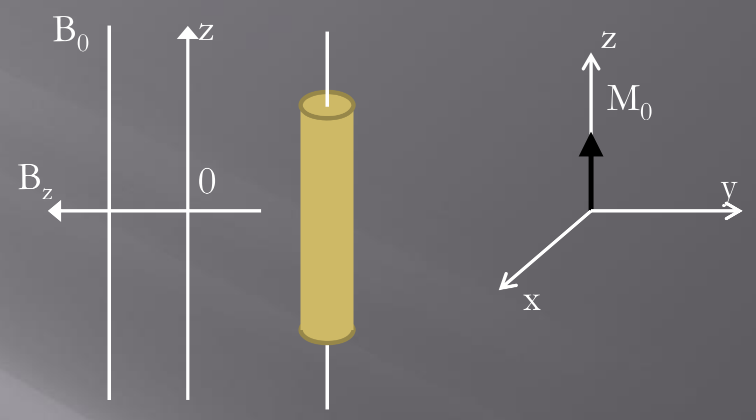

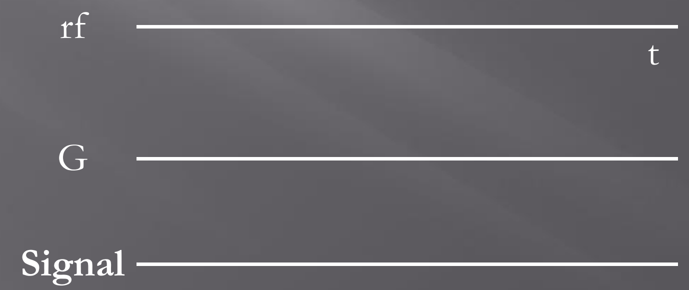

Applying an oscillating rf field along the x-axis rotates M_0 from the z-axis into the transverse plane so that it lies along the y-axis.

At this time, the rf field is turned off and the transverse magnetization precesses about the main field B_0.

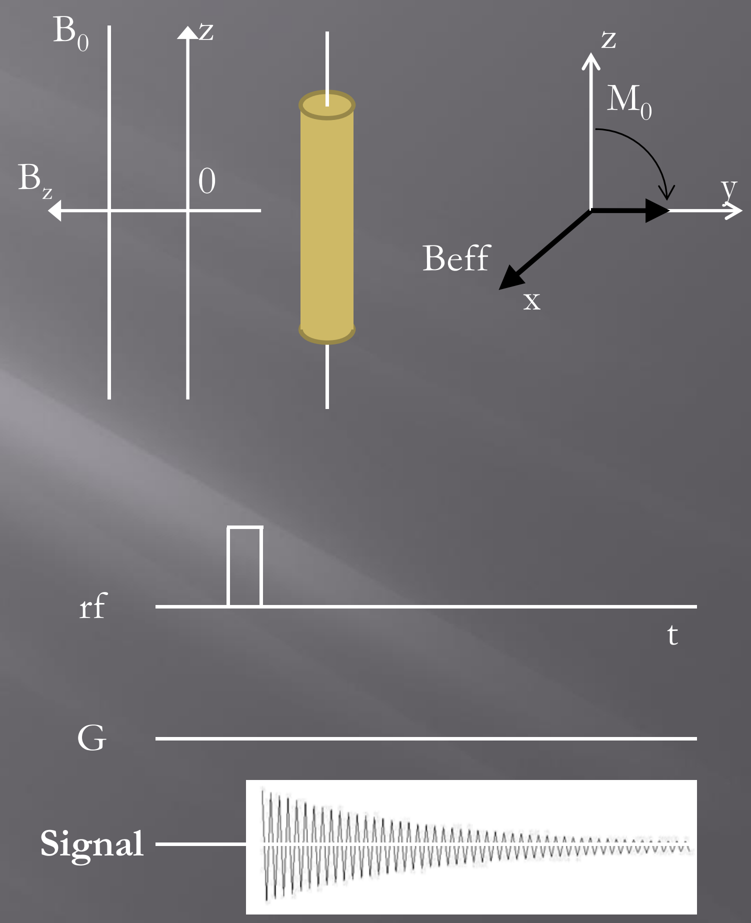

MR Signal Readout

The precessing transverse component induces a voltage in a coil which is placed so that it sees a changing magnetic flux.

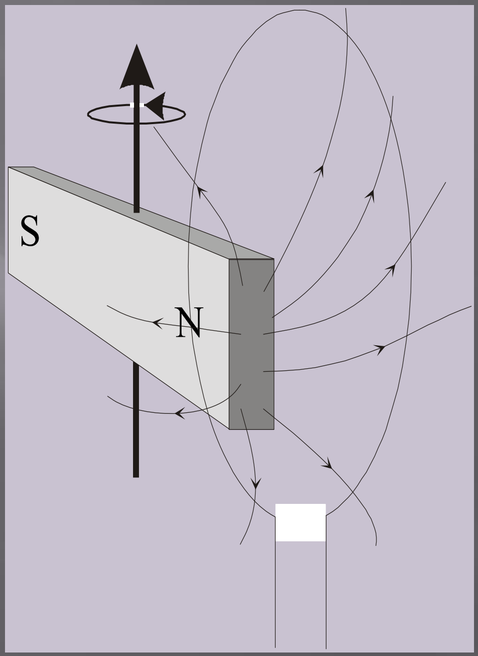

Gradient Echoes and 1D Imaging

The Larmor equation

- $\boldsymbol{\omega} = -\gamma B$
- $\phi = \omega t$
- $\phi = -\gamma B t$
  - Right-handed system
  - γ: gyromagnetic ratio.
  - For hydrogen,

    $\bar{\gamma} = \gamma/2\pi = 42.576\ \mathrm{MHz \cdot T^{-1}}$

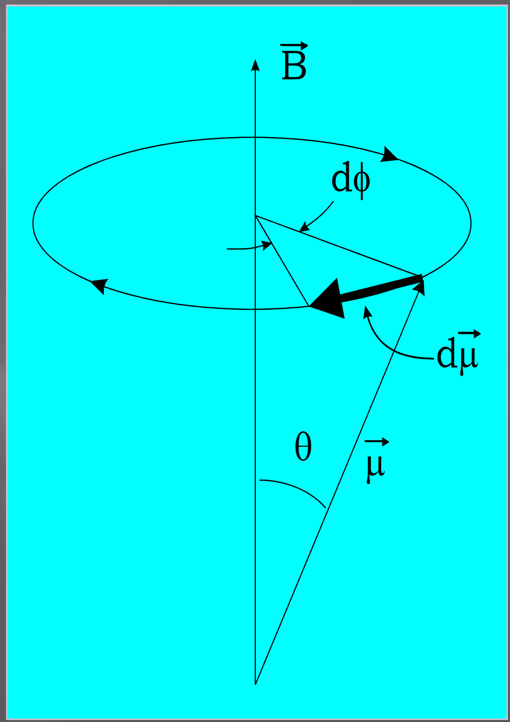

By purposely adding a gradient field G, we can spatially distinguish the spins by their frequency content since now

$$\omega(x) = \gamma\,(B_0 + Gx)$$

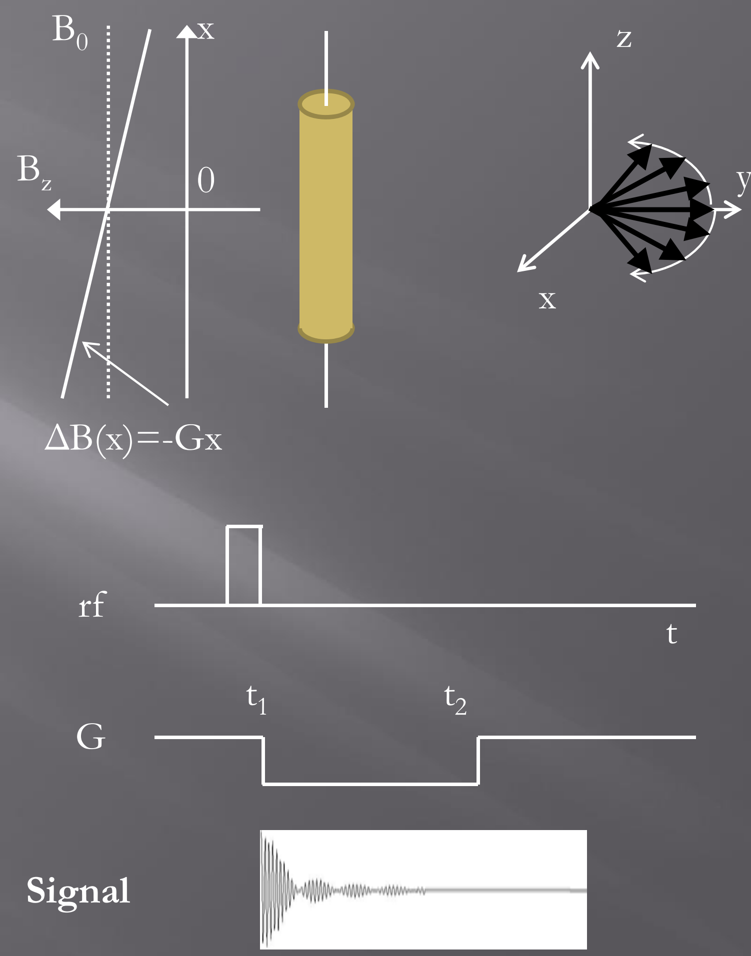

Applying a dephasing gradient followed by a rephasing gradient causes the spins to first run away from each other and then to turn around and run back creating a gradient echo.

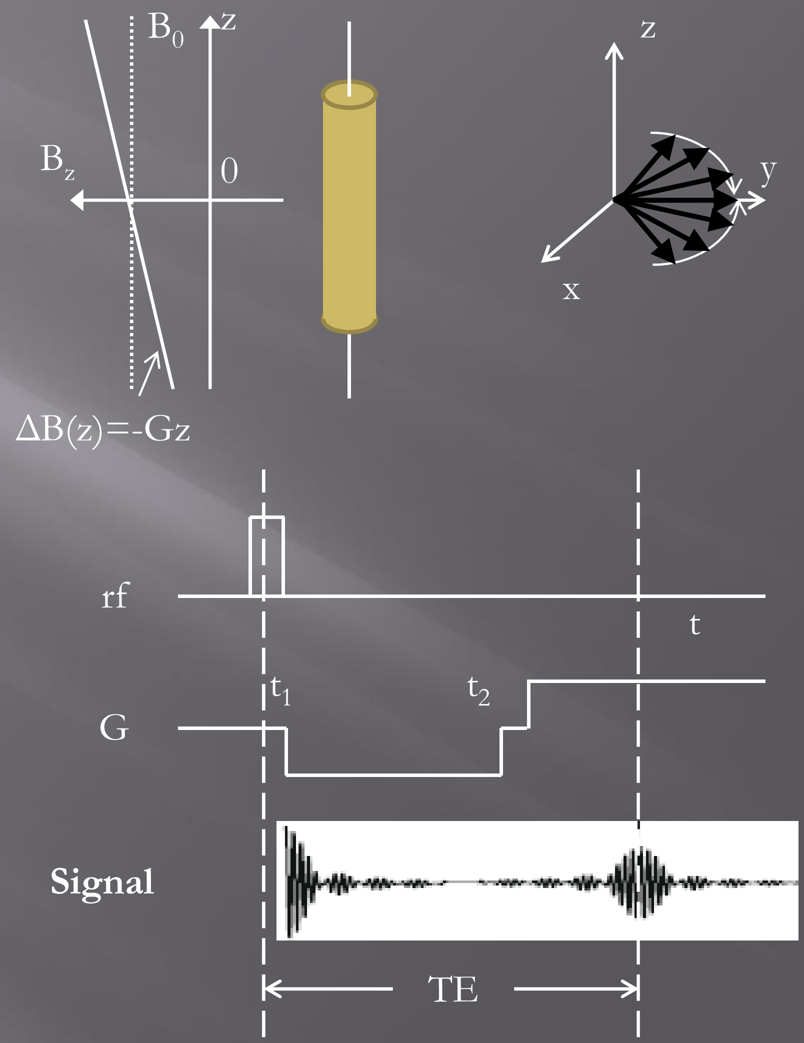

The MR Signal as a Fourier Transform

$$s(t) = \int dx \rho(x) \mathrm{e}^{-i\gamma G x t}$$

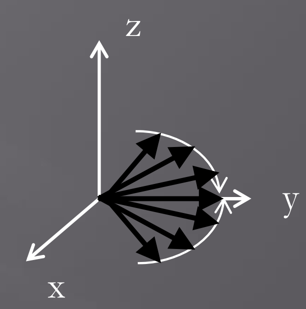

where $\rho(x)$ is the spin density and using $k = \gamma Gt$ as the spatial frequency we find

$$s(k) = \int dx \rho(x) \mathrm{e}^{-i2\pi k x}$$

the spin density can be reconstructed as

$$\rho(x) = \int dk s(k) \mathrm{e}^{i2\pi k x}$$

Phase Evolution

- Phase is the integral of precession frequency (or field strength) over time

$$\phi(t) = \int dt\, \omega(t)$$

$$\omega = \gamma \Delta B_z$$

$$\phi(t) = \gamma \int dt\, \Delta B_z(t)$$

- Gradients
- Susceptibility Induced Fields
- Eddy Currents
- Main Field Inhomogeneities
- Molecular Environment (Chemical Shift)

Phase of Gradient-echo Signal

- The complex MRI signal has both real and imaginary components or magnitude and phase components
- $\varphi(TE) = \gamma \Delta B \cdot TE + \varphi_{0,}$ for a left-handed system.

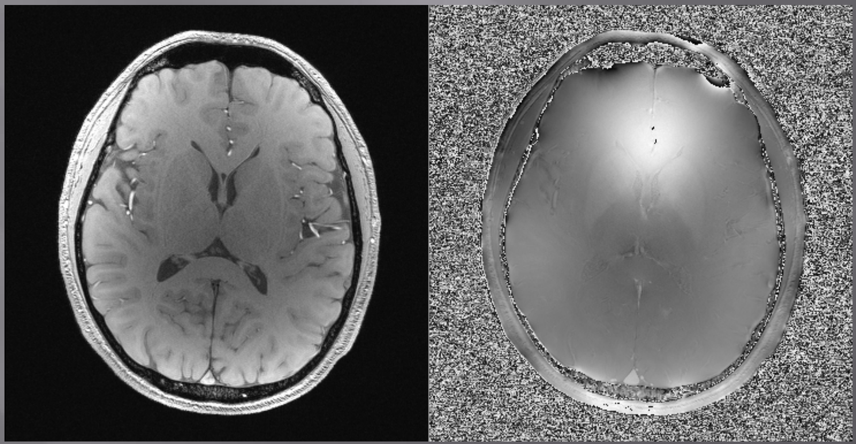

[1]Magnitude Image Phase Image

[1]Data were acquired using 3D gradient-echo sequence with full flow compensation (SWI sequence).

Effect of Bandwidth on MR image Quality

Bandwidth 110 Hz/Px

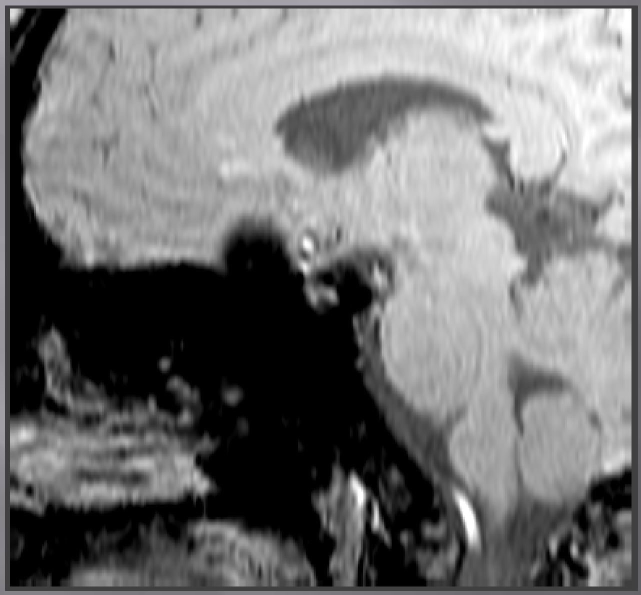

Bandwidth 473 Hz/Px

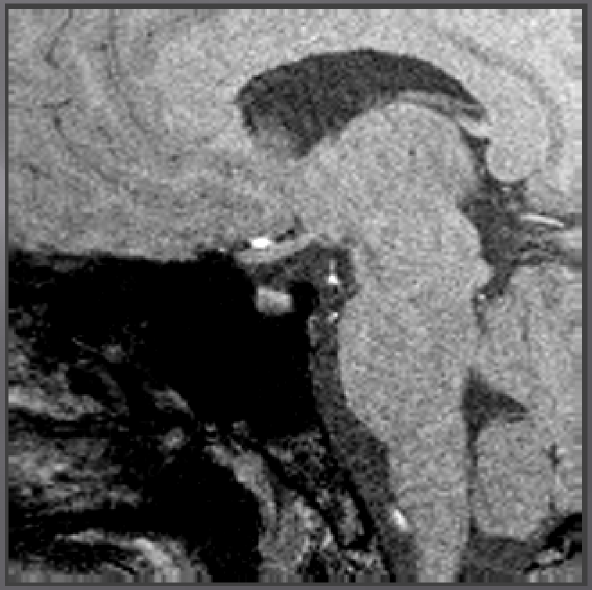

Effect of TE on MR image Quality

TE=10ms

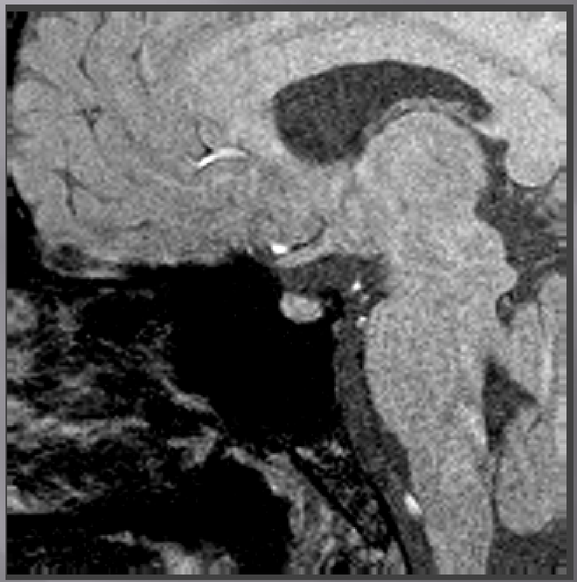

0.7x0.7x1.4mm^3

TR=14ms, Flip angle:12°

Bandwidth=473 Hz/Px

$\phi = \gamma \Delta B t$

TE=2.5ms

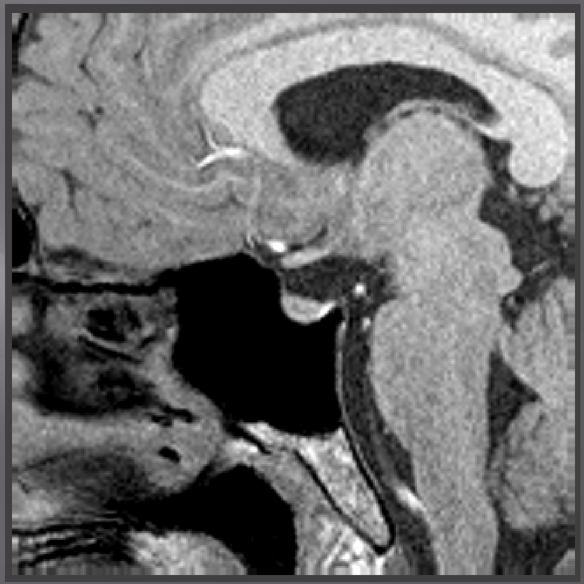

0.7x0.7x1.4mm^3

TR=14ms, Flip angle:12°

Bandwidth=473 Hz/Px

Signal Decay Due to Phase Dispersion Across a Voxel

Spins	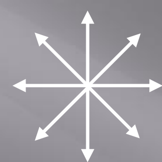	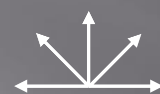		
$\Delta\boldsymbol{\theta}$	2π	$\boldsymbol{\pi}$	$\boldsymbol{\pi}/2$	0
sinc($\Delta\theta$/2)	0	$\mathbf{\frac{2}{\pi}}$	$\mathbf{\frac{2\sqrt{2}}{\pi}}$	1
Signal	0	$64\%\rho_0$	$90\%\rho_0$	ρ_0

$$\rho(x) = \rho_0\left[\frac{1}{\Delta\theta}\int_{-\Delta\theta/2}^{\Delta\theta/2} e^{i\varphi}\, d\varphi\right] = \rho_0 sinc(\Delta\theta/2)$$

Phase Dispersion at Different TEs

- Phase dispersion across a voxel leads to signal decay and hence low intensity on magnitude images

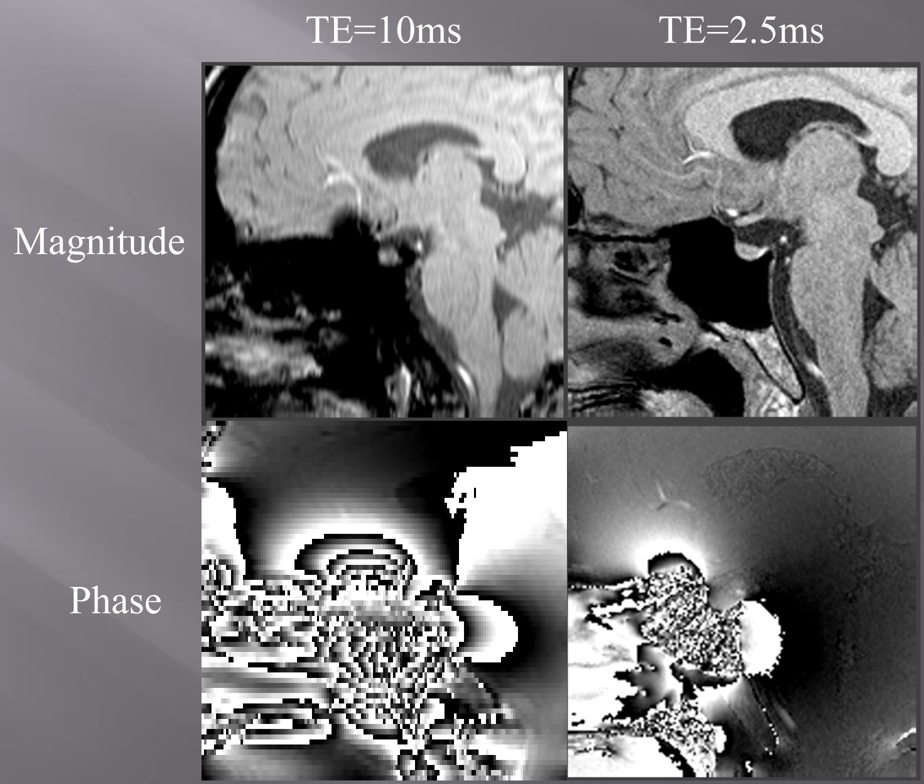

Phase Unwrapping

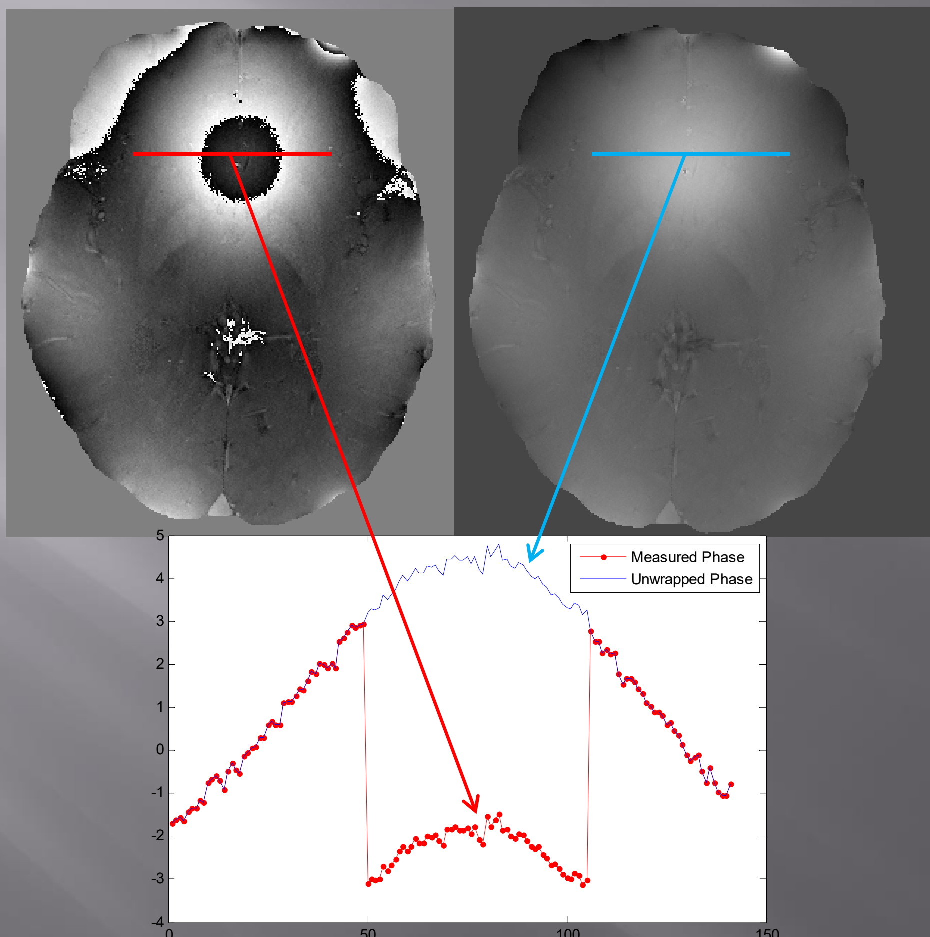

- $\varphi_{act}(r)_{=}\varphi_{measured}(r)+2\pi\cdot n(r)$
- The goal of phase unwrapping is to determine the function n(r) to remove the discontinuities in the measured phase.
- Algorithms
  - spatial domain, based on the smoothness assumption of the phase in single-echo data
  - temporal domain, using the small phase increment in multi-echo data

Phase Unwrapping

- Spatial domain algorithms
  - Assuming smooth spatial profile of phase
  - Failure due to phase singularities/cusp artifacts or violation of the smoothness assumption
  - ΦUN[1], Prelude in FSL[2], 3D-SRNCP[3], Laplacian method
- Temporal domain algorithms
  - Utilizing the short echo spacing in multi-echo data
  - Requires 3 or more echoes
  - Time-efficient for pixel by pixel phase unwrapping
  - CAMPUS[4], UMPIRE[5]

[1]Witoszynskyj S. et al. Med Image Anal. 2009;13(2):257-68.
[2]Jenkinson, M. Magn Reson Med. 2003; 49: 193–197.
[3]Abdul-Rahman HS. et al. Appl Opt. 2007;46(26):6623-35.
[4]Feng W. et al. Magn Reson Med. 2013;70(1):117-26.
[5]Robinson S. et al. Magn Reson Med. 2014;72(1):80-92.

Complex Division and the Effective Echo Time

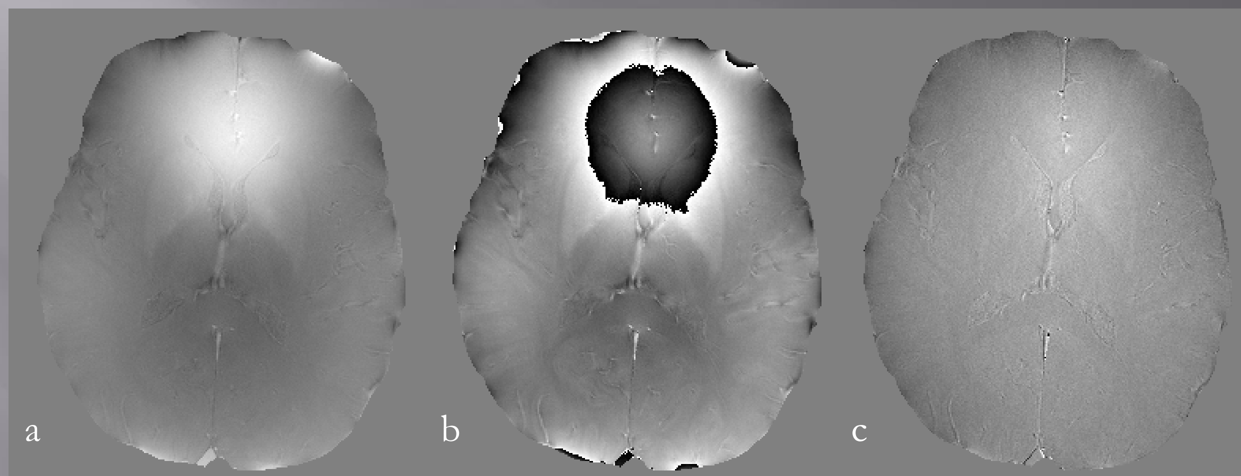

TE_1=7.38ms TE_2=17.6ms $\Delta TE = TE_2 - 2TE_1 = 2.84$ms

- $\varphi(\Delta TE) = \arg\{\exp[i(\varphi(TE_2) - 2\,\varphi(TE_1))]\}$
- Phase unwrapping is not necessary for the phase images at the short effective echo time.

Background Field Removal Algorithms

Comparison of the phase images processed with different algorithms

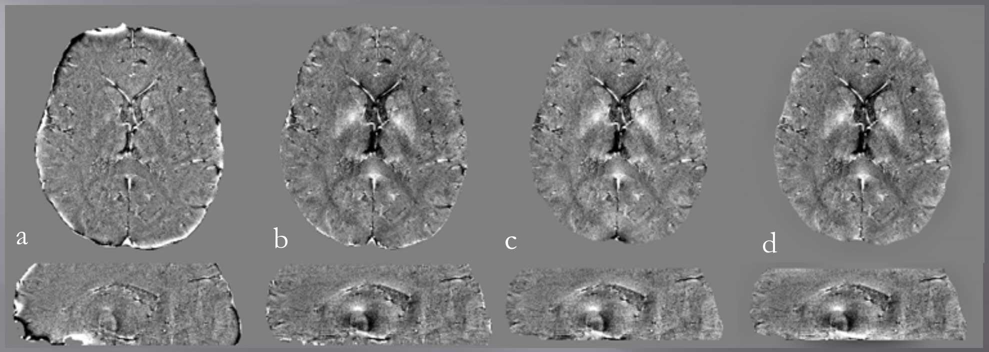

e
[1]Homodyne High-pass filter

f
[2]Variable High-pass filter

g
[3]SHARP

h
[4]PDF

Effects of different background field removal algorithms on susceptibility quantification

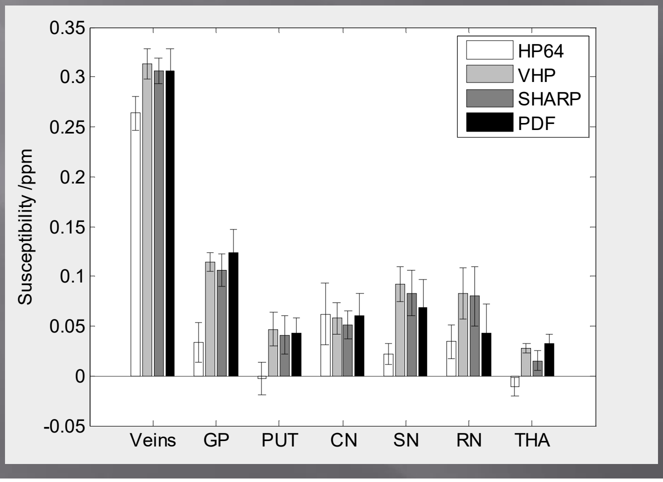

1. Haacke, E.M., et al. Magn Reson Med. 2004;52(3):612-8.
2. Haacke, E.M., et al. Magn Reson Imaging. 2015;33(1):1-25.
3. Schweser, F., et al. Neuroimage. 2011;54(4):2789-807.
4. Liu, T. et al, NMR Biomed. 2011;24(9):1129-36.

Water Fat Separation

- $\omega = \gamma B_0(1-\sigma)$
  - σ is the shielding constant.
- $\rho(TE) = \left(\rho_w + \rho_f e^{-i\Delta\omega_{fw}TE}\right)e^{-i\gamma\Delta B\cdot TE - i\phi_0}$
  - $\Delta\omega_{fw} = -\sigma_{fw}\gamma B_0$, where σ_{fw} is the chemical shift between fat and water, which is 3.35ppm for most fat in the body.
  - ϕ_0: phase related to rf penetration or tissue conductivity.

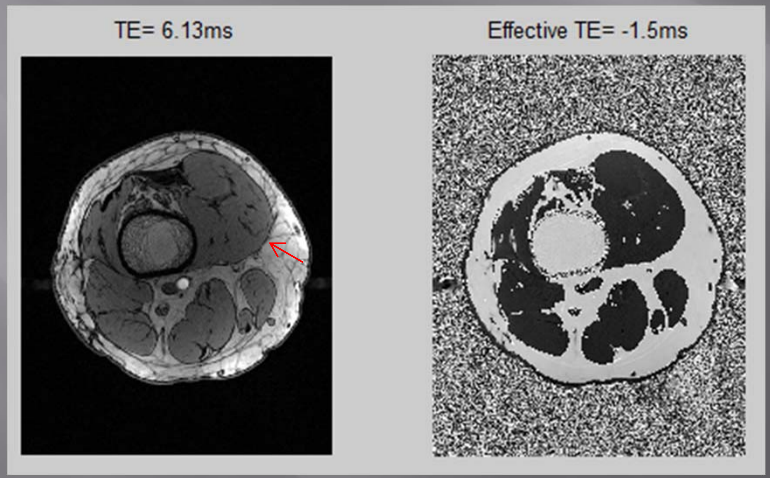

Transverse view of the magnitude (left) and complex divided phase (right) images of the leg at different echo times. The phase images were generated by complex dividing the original phase at TE=7.63ms into the original phase images at other TEs.

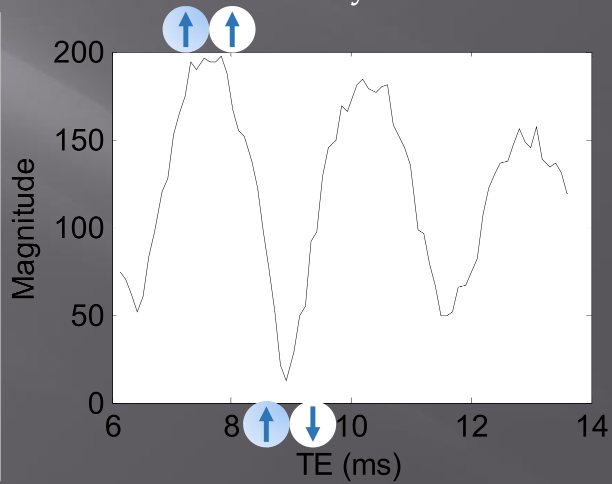

The beating envelope of the magnitude as a function of TE for one voxel containing both water and fat, as indicated by the red arrow.

Water Fat Separation

Original phase evolution for a pixel contains water

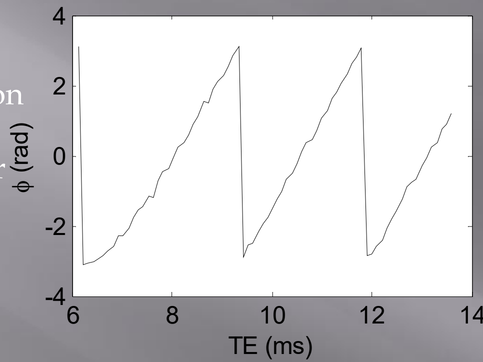

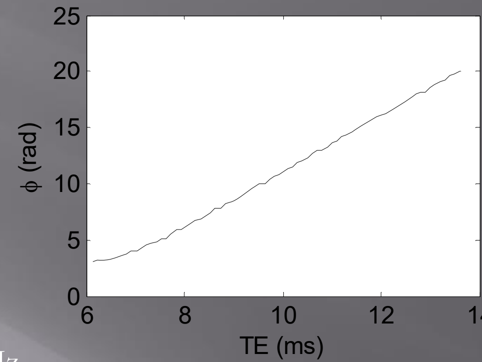

Unwrapped phase evolution for a pixel contains water

Frequency Map ($\gamma\Delta B$) obtained from a simple linear fitting using the unwrapped phase at all the echoes, followed by 2D quadratic fitting to remove field variation induced by the global geometry.

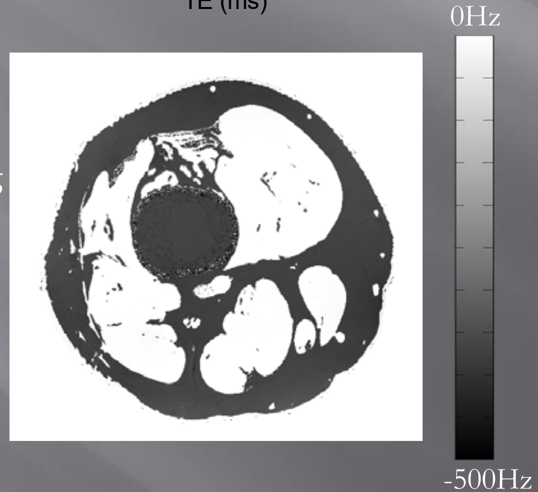

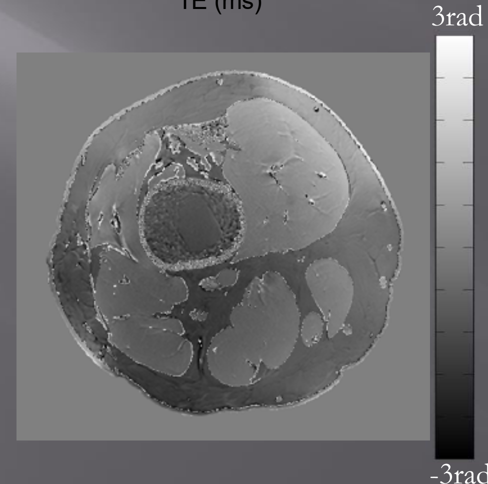

ϕ_0 Map. The values were wrapped into the range of –π to π.

Considering the both the frequency difference between water and fat and the phase difference seen in the ϕ_0 map (due to the difference in conductivity), the water/fat in-phase echo times at 3T were found to be 2.66·N-0.30 ms, where N=1, 2, 3…

Three-point Water Fat Separation

- ρ_w, ρ_f, ΔB and ϕ_0 can be determined using two water/fat in-phase echo times (TE_1 and TE_3), and on water/fat opposed-phase echo time (TE_2) [1, 2].
- $$\begin{cases} \rho(TE_1) = (\rho_w + \rho_f)e^{-i\gamma\Delta B\cdot TE_1 - i\phi_0}e^{\frac{TE_1}{T_2^*}} & [1] \\ \rho(TE_2) = (\rho_w - \rho_f)e^{-i\gamma\Delta B\cdot TE_2 - i\phi_0}e^{\frac{TE_2}{T_2^*}} & [2] \\ \rho(TE_3) = (\rho_w + \rho_f)e^{-i\gamma\Delta B\cdot TE_3 - i\phi_0}e^{\frac{TE_3}{T_2^*}} & [3] \end{cases}$$
- $$\Delta B = \frac{[\phi(TE_3) - \phi(TE_1)]}{-\gamma(TE_3 - TE_1)} \quad [4]$$
  - Phase unwrapping may be required
- $$\phi_0 = -[\phi(TE_1) + \gamma\Delta B \cdot TE_1] \quad [5]$$
- $$\hat{\rho}_{in} = \frac{1}{2}(|\rho(TE_1)| + |\rho(TE_3)|) \quad [6]$$
  - To compensate for the effects due to T2* decay
- $$\hat{\rho}_{op} = \rho(TE_2)e^{i\Delta B\cdot TE_2 + i\phi_0} \quad [7]$$
- $$\hat{\rho}_w = \frac{1}{2}(\hat{\rho}_{in} + \hat{\rho}_{op}),\ \hat{\rho}_f = \frac{1}{2}(\hat{\rho}_{in} - \hat{\rho}_{op}) \quad [8]$$

Water Fat

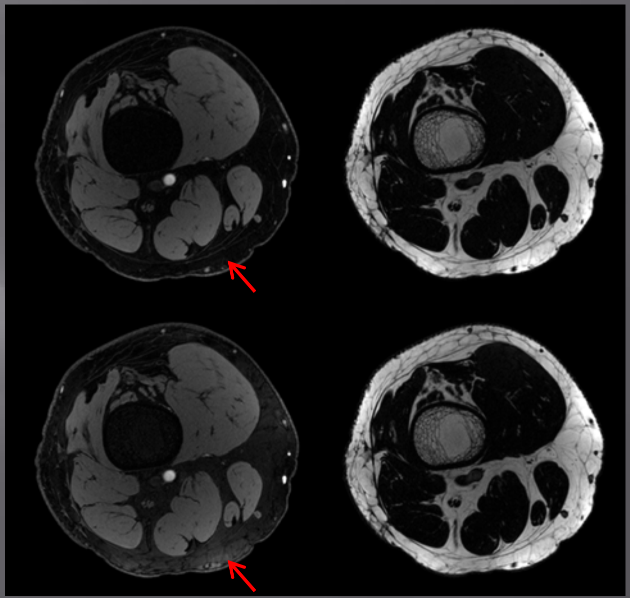

1st row: Three-point method;
2nd row: Two-point method using images at one in-phase and another opposed-phase echo times.

1. Haacke, EM, Patrick JL, Lenz GW, Parrish T. The separation of water and lipid components in the presence of field inhomogeneities. Rev Magn Reson Med 1986;1:123–154.
2. Glover, G. H., and Schneider, E., Magn Reson Med, 1991,18: 371–383.

Flow Quantification

- Some quick math behind this…
  - The phase of a spin with initial position x and velocity v is given as

    $$\phi = \phi_0 + \gamma x M_0 + \gamma v M_1 \quad [1]$$

    M_n refers to the n^{th} order moment of the gradient over time. ϕ_0 is background phase.

  - For a bipolar gradient, $M_0=0$ and $M_1 \neq 0$.

    $$\phi = \phi_0 + \gamma v M_1 \quad [2]$$

    <u>Phase is now a function of velocity</u>

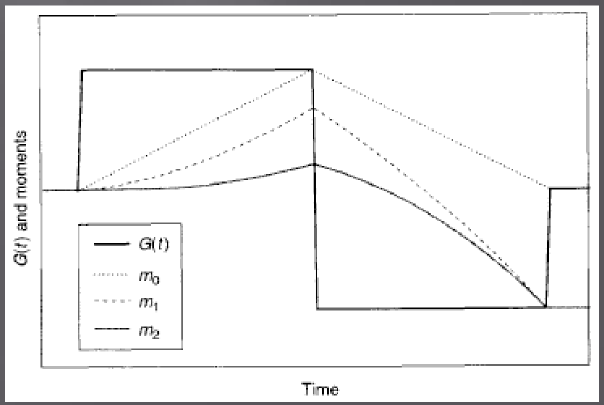

Phase Aliasing in Flow Quantification

- If v=±venc, then $\varphi=\pm\pi$… What if v>|venc|?
  - This causes "***phase aliasing***".
  - Here a Venc of 50cm/sec was too small.

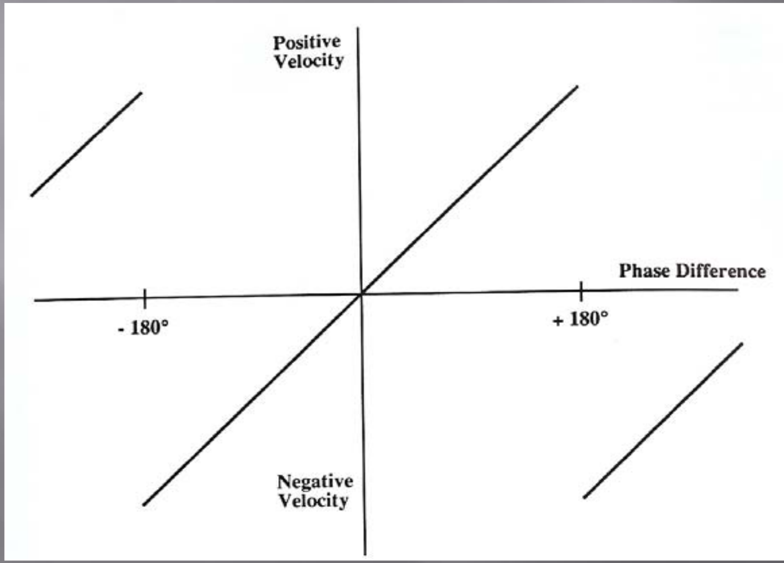

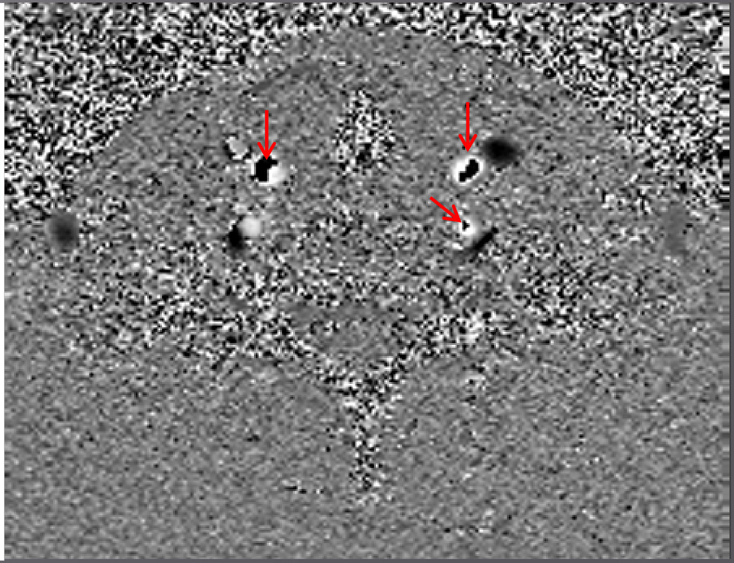

Flow Change During a Given Cardiac Cycle

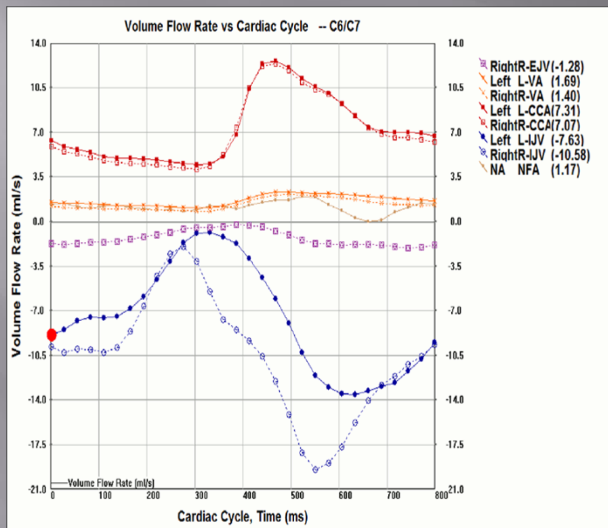

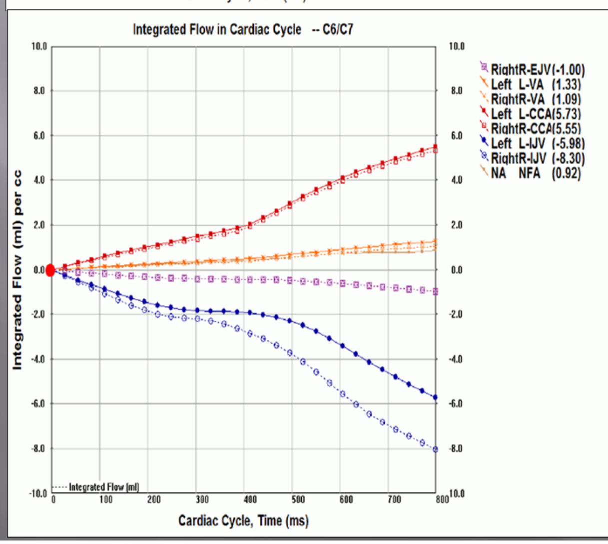

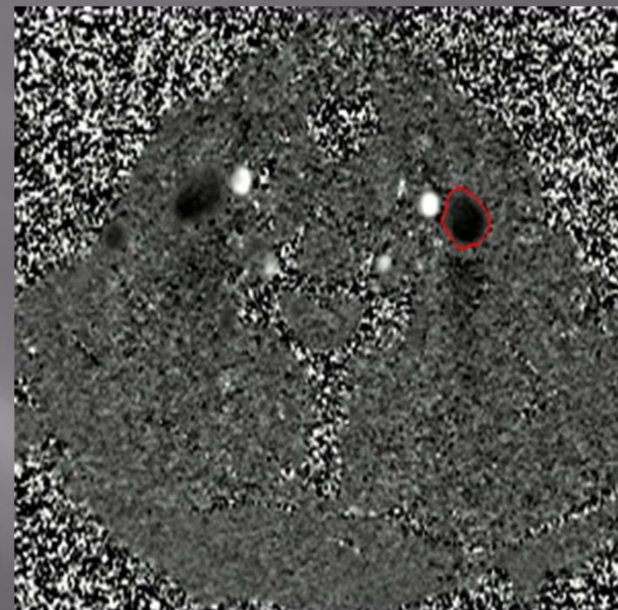

Flow rate and integrated flow for the right internal jugular vein (RIJV). The red circle follows the darkening of the signal in the phase image above.

MR Thermometry

- $\omega = \gamma B_0(1-\sigma)$ [1]
  - σ is the shielding constant.
- $\sigma = \alpha T$ [2]
  - T: temperature
  - α~0.01ppm/°C [1]
- $\phi(T) = \gamma[\Delta B - \alpha T B_0] \cdot TE + \phi_0$ [3]
  - By measuring the phase at T and reference temperature $T_{0,}$ T can be determined from the phase difference image[2].
- $T = [\phi(T_0) - \phi(T)](\alpha\gamma B_0 TE)^{-1} + T_0$ [4]

[1]Ishihara, Y. et al., MRM (1995), 34:814-823.
2 Rieke, V., and Pauly, KB. JMRI (2008), 27:376-390.

Phase and Field Inhomogeneity

- Phase is proportional to field inhomogeneity:
  - $\phi(r) = -\gamma \Delta B(r) TE + \phi_0$
  - Right-handed system, gradient-echo data
- Field variation and susceptibility distribution
  - $\Delta B_z(\vec{r}) = \frac{\mu_0}{4\pi} \int_{V'} d^3 r' \{ \frac{3 M_z(\vec{r}')(z-z')^2}{|\vec{r}-\vec{r}'|^5} - \frac{M_z(\vec{r}')}{|\vec{r}-\vec{r}'|^3} \}$ [1]
  - $\Delta B(r) = B_0 \cdot G(r) * \Delta\chi(r)$ [2]
  - $G(r) = \frac{1}{4\pi} \cdot \frac{3\cos^2\theta - 1}{r^3}$ [3]

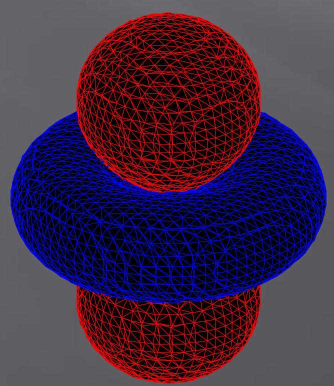

Orientation Dependence

$$\varphi(r, TE) = -\gamma \Delta B(r) T_E$$

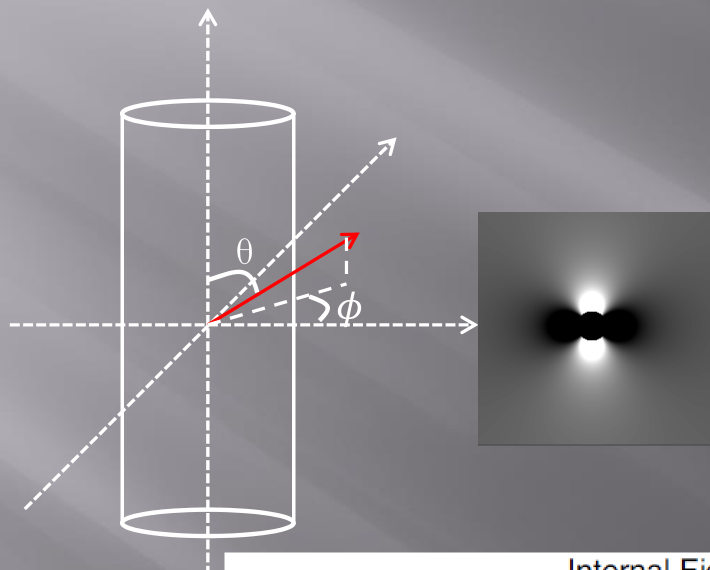

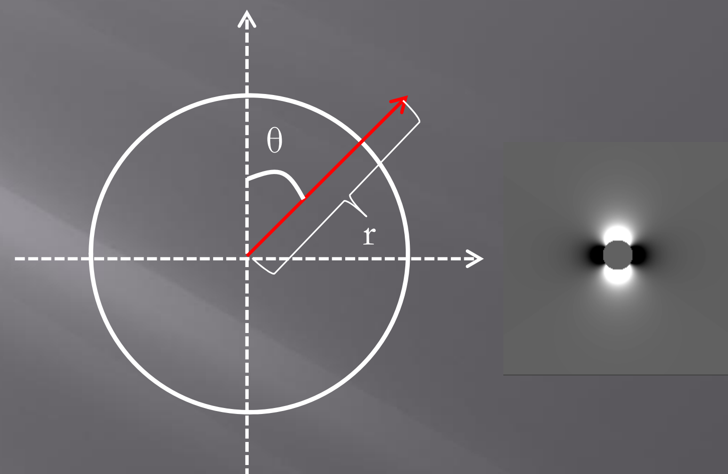

	Internal Field	External Field
Sphere	B_0	$B_0 + \frac{\chi B_0}{3} \cdot \frac{a^3}{\lvert\mathbf{r}\rvert^3} \cdot (3\cos^2\theta - 1)$
Cylinder	$B_0 + \frac{\chi B_0}{6} \cdot (3\cos^2\theta - 1)$	$B_0 + \frac{\chi B_0}{2} \cdot \frac{a^2}{\lvert\mathbf{r}\rvert^2} \sin^2\theta \cos 2\phi$

Haacke et al. Susceptibility weighted imaging in MRI: p29

Microbleeds in RHS vs. in LHS

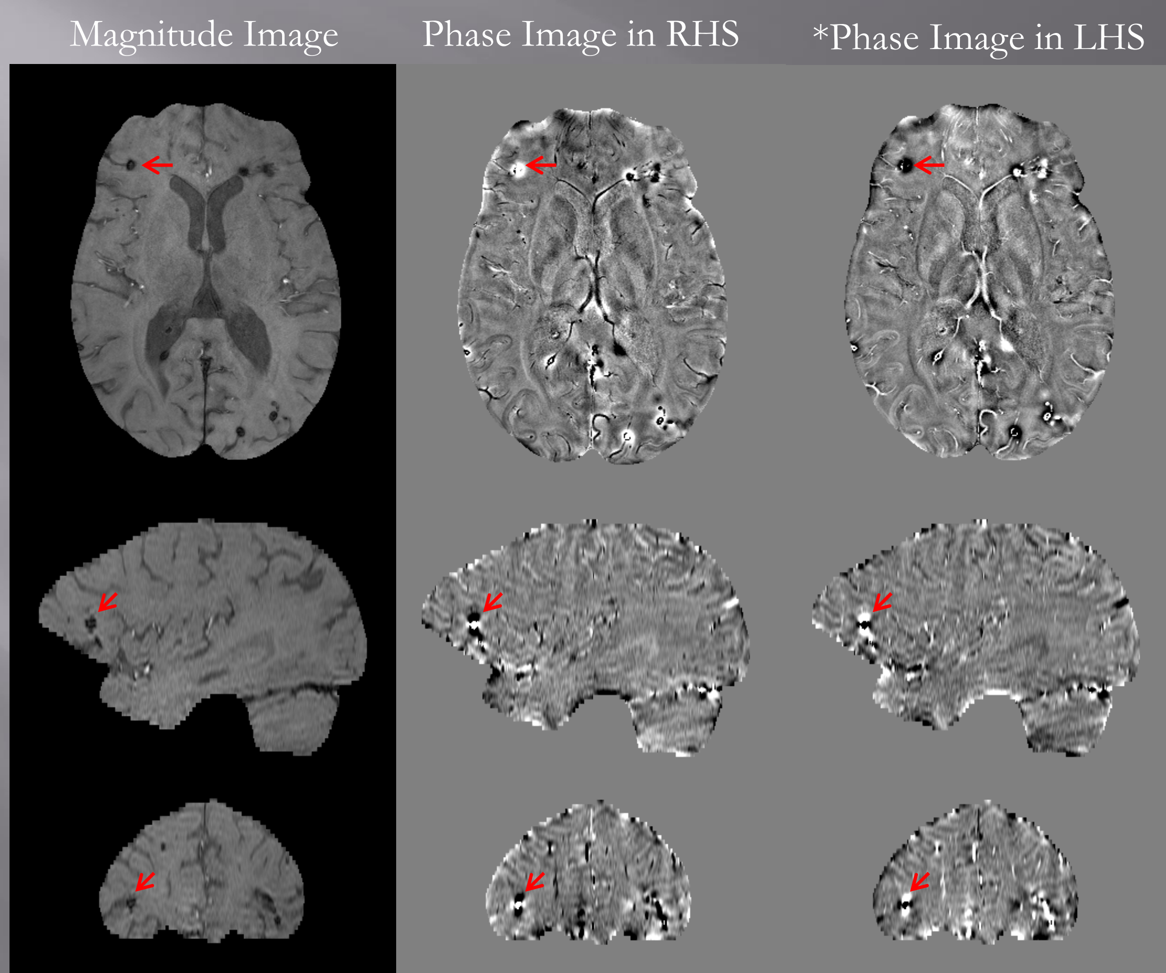

Field variation induced by a spherical object for a LHS

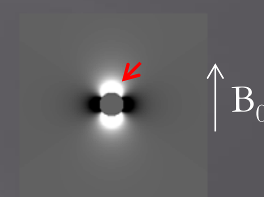

*Phase Image were processed using 64x64 Homodyne high-pass filter. Images in sagittal and coronal views were interpolated to isotropic resolution for better visualization.

Background Field Removal using the Forward Field Prediction

Sinus map

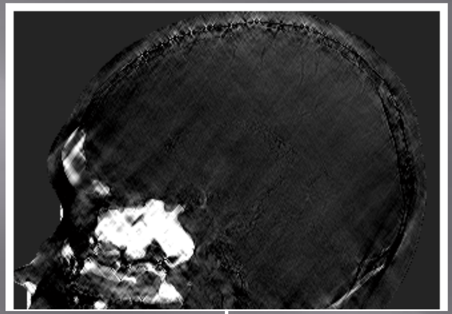

Forward Prediction

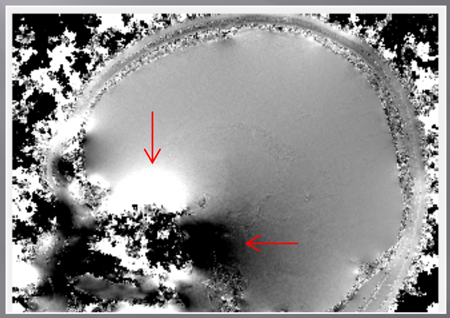

−

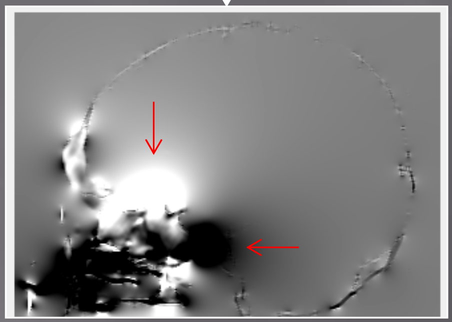

=

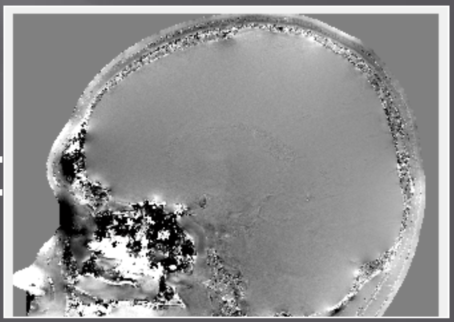

Original unwrapped phase

Predicted phase

Corrected phase

Multi-channel data combination and phase images reconstruction

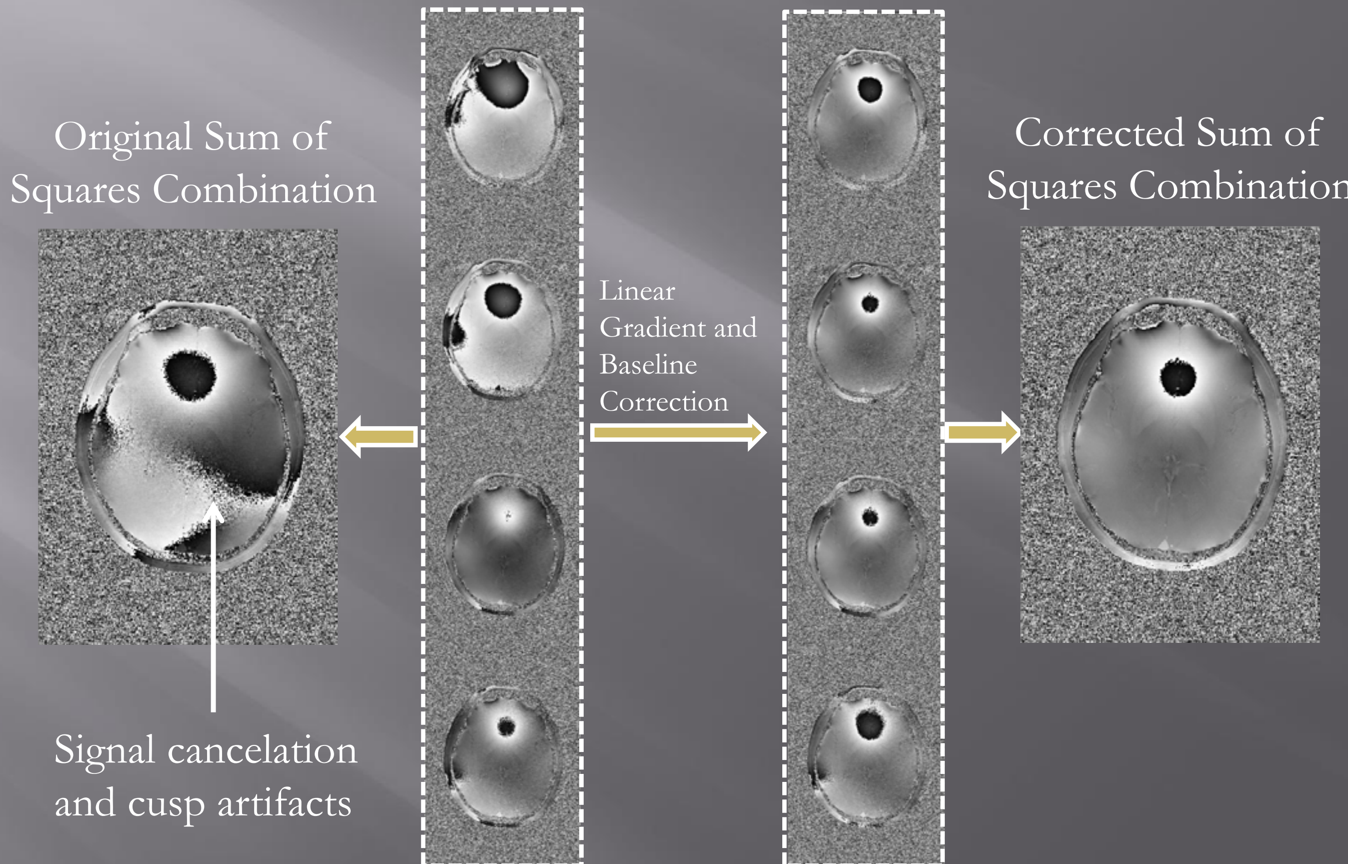

E-poster 3309, 16:30, June 1st

Complex Division for Phase Unwrapping

- If the ultimate goal is to determine the local field variation, instead of the original field which also includes the background field, pixel-by-pixel phase unwrapping may be viable.

$\Delta TE = TE_2 - 2TE_1 = 2.84\text{ms}$

$TE_1 = 7.38\text{ms}$ | $TE_2 = 17.6\text{ms}$

Original Phase Images

After Background Phase Removal

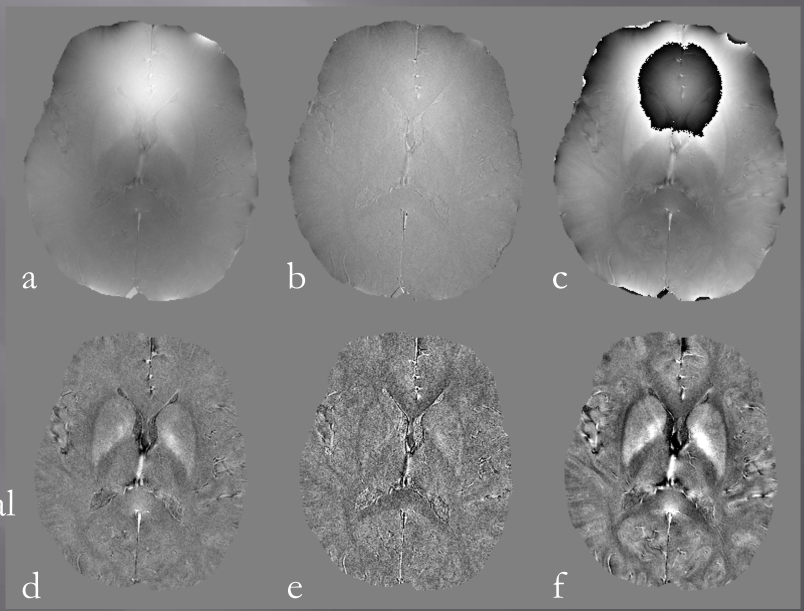

Generated from a | Generated from b | Generated as 2×d+e

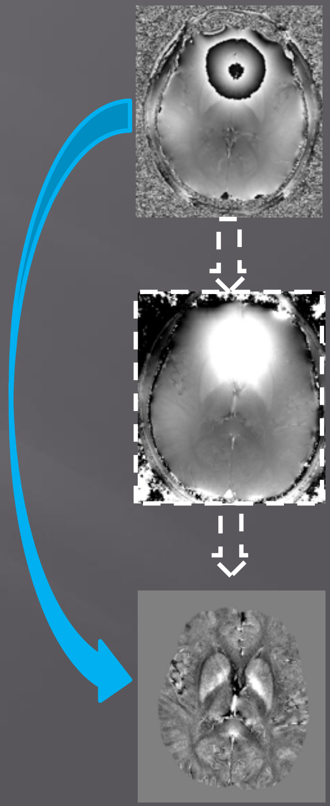

Overview of the Data Processing Steps in SWI and QSM

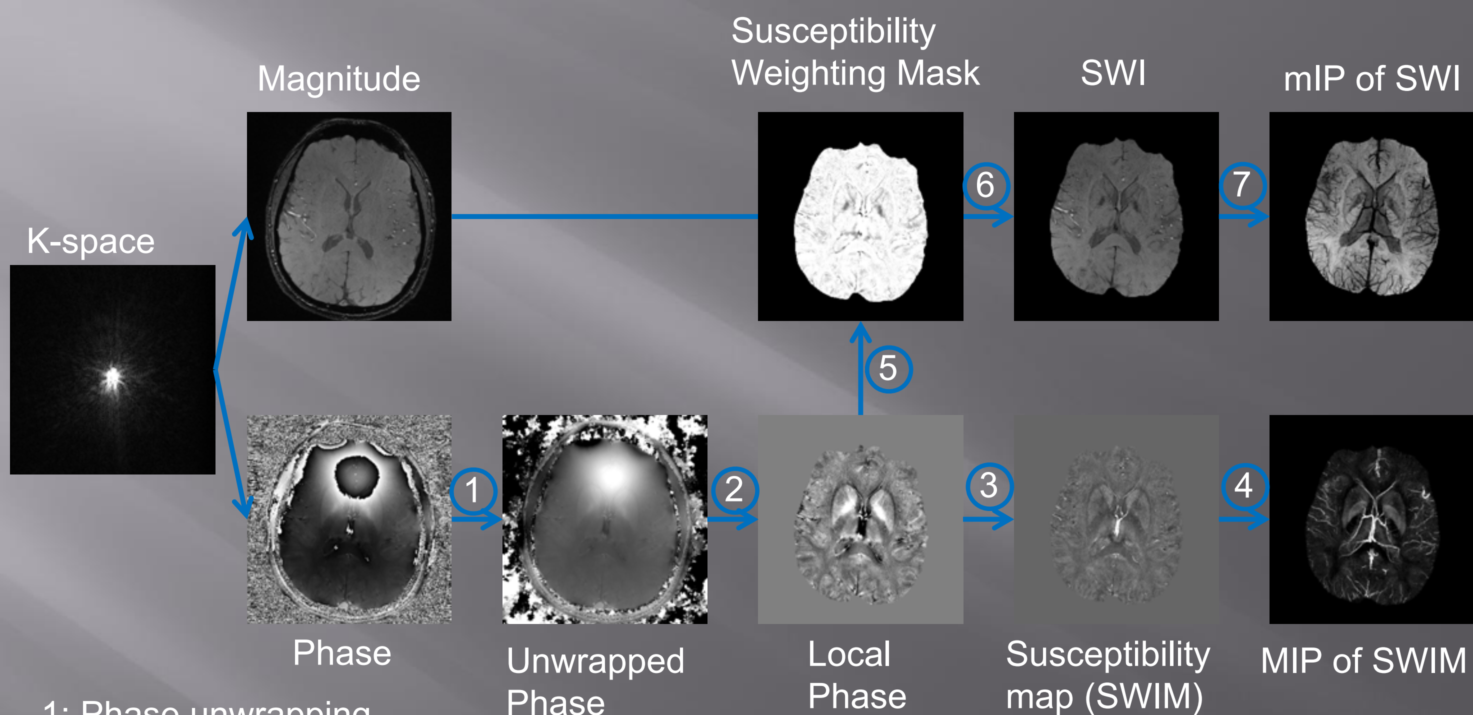

1: Phase unwrapping.
2. Background phase removal.
3. Susceptibility mapping by solving the inverse problem.
4. Maximum Intensity Projection (MIP).
5. Generating the susceptibility weighting mask.
6. Multiplication of original magnitude image with the susceptibility weighting mask.
7. Minimum Intensity Projection (mIP).

Phase MIP versus QSM MIP?

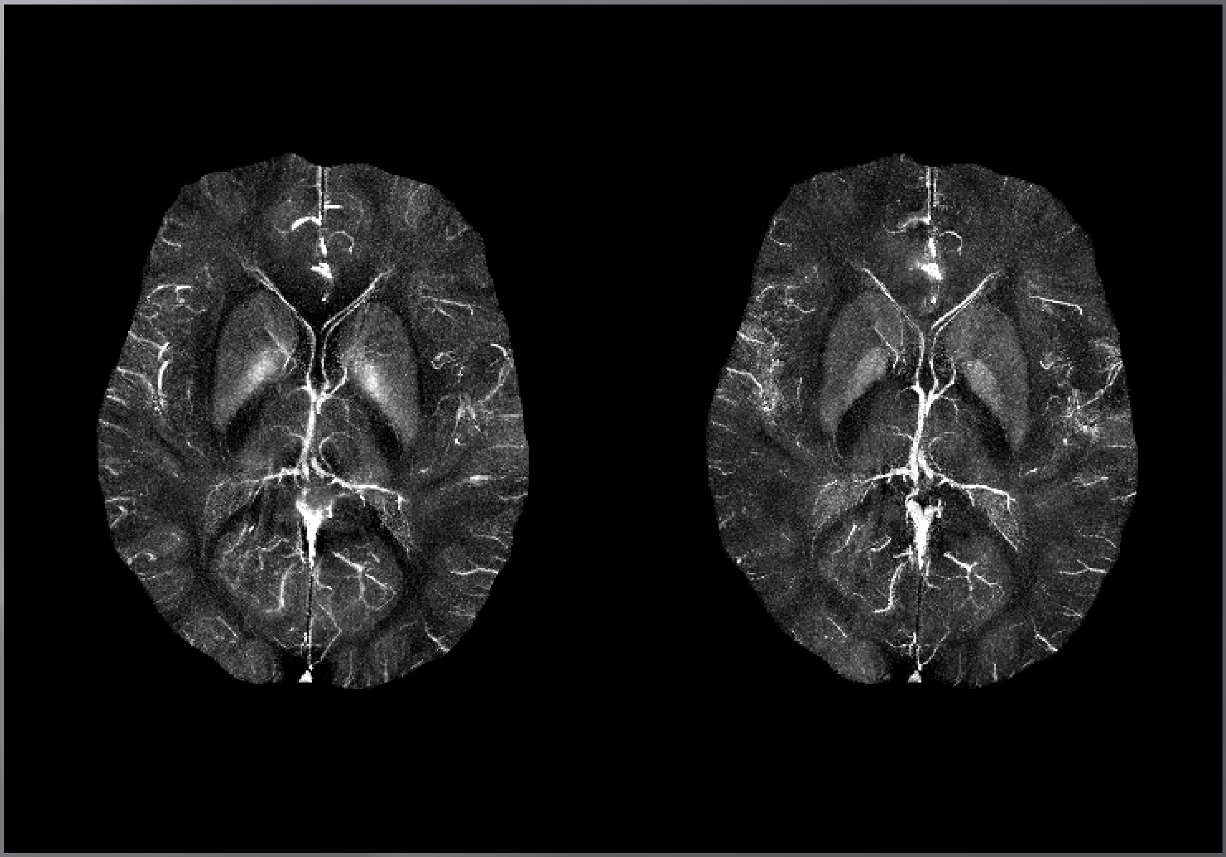

Iron Mapping in Normal Volunteers using QSM

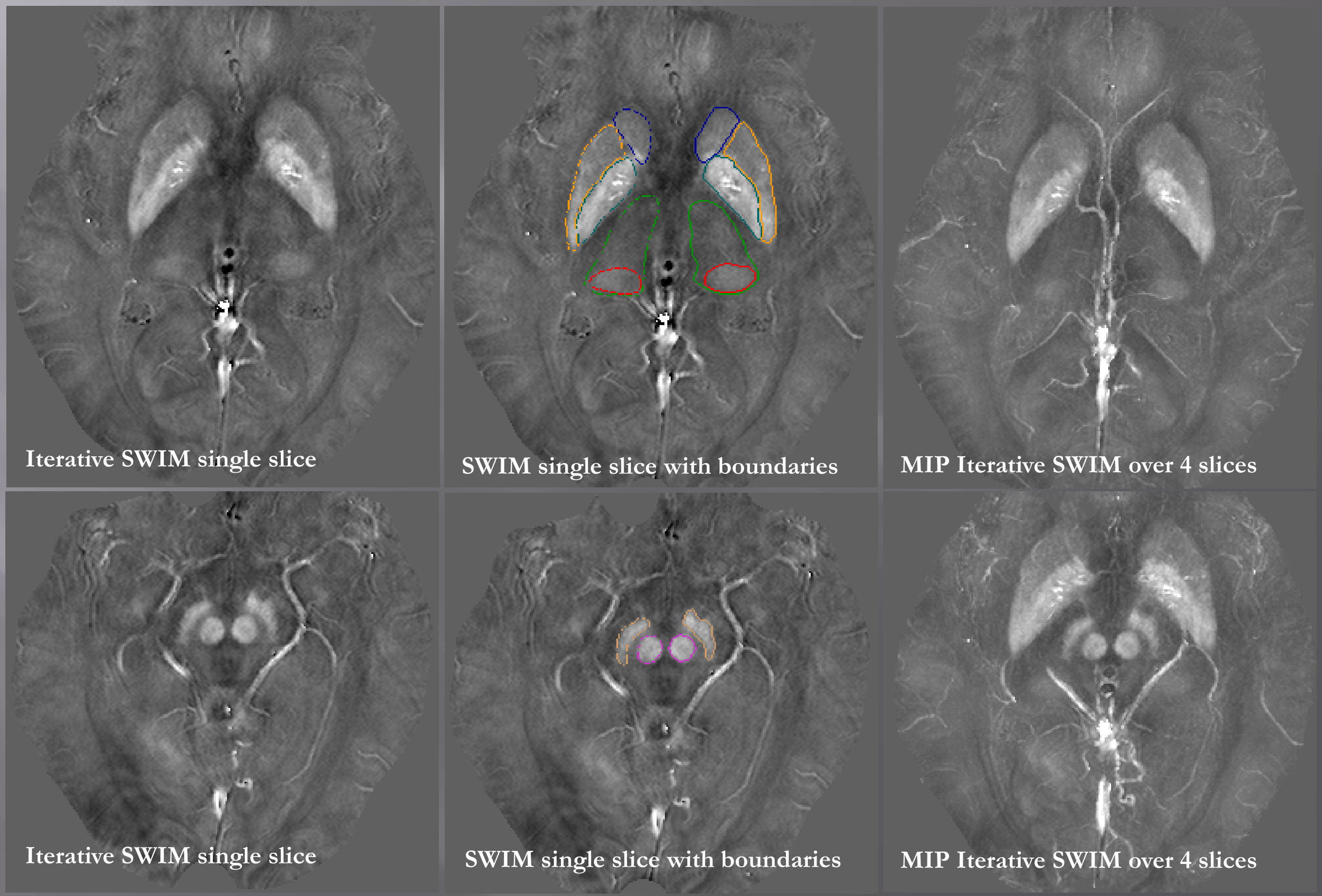

Whole brain iron and oxygen saturation using quantitative susceptibility mapping

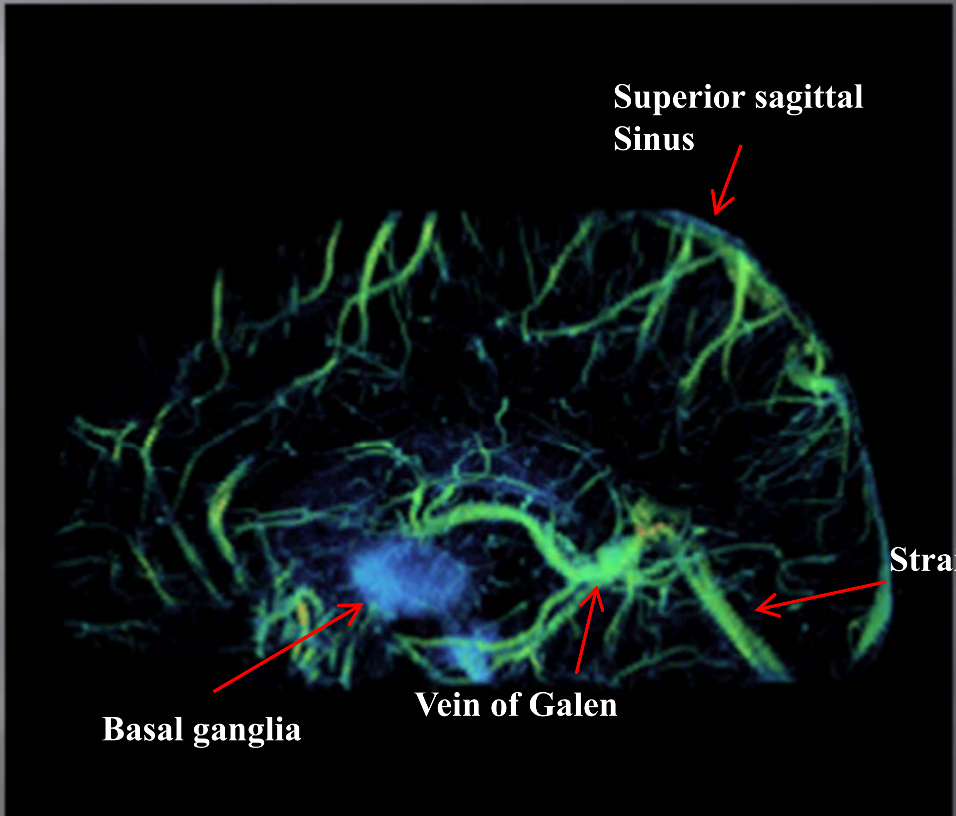

Green - deoxyhemoglobin levels in the veins

Blue represents iron in the basal ganglia and midbrain

Conductivity Mapping

- Conductivity and permeability can be reconstructed using the RF transmit field (or receive field) through Helmholtz equation[1-3]:

$$\frac{\nabla^2 B_1^+}{B_1^+} = -(\mu_o \varepsilon \omega + i\mu_o \omega \sigma)$$

  - B_1^+: complex transmit field. μ_o: permeability. σ: conductivity.
  - We can find ε and σ using the magnitude and phase data.

[1]Haacke EM et al. Phys. Med. Biol. 1991;36:723-734.
[2]van Lier AL. et al, Magn Reson Med. 2014;71(1):354-63.
[3]Marques JP. et al., Magn Reson Med. 2014. doi: 10.1002/mrm.25399.

EPT for *in vivo* brain conductivity

- investigate brain conductivity quantitatively *in vivo* with phase-based EPT
- correlation between conductivity and malignancy of brain tumors (Courtesy of Ulrich Katscher)

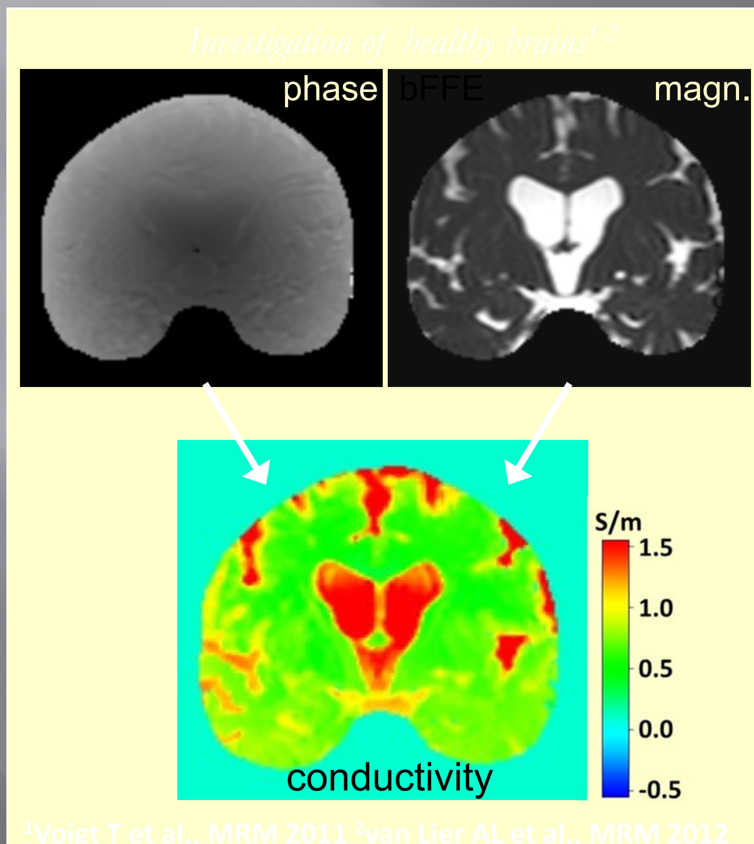

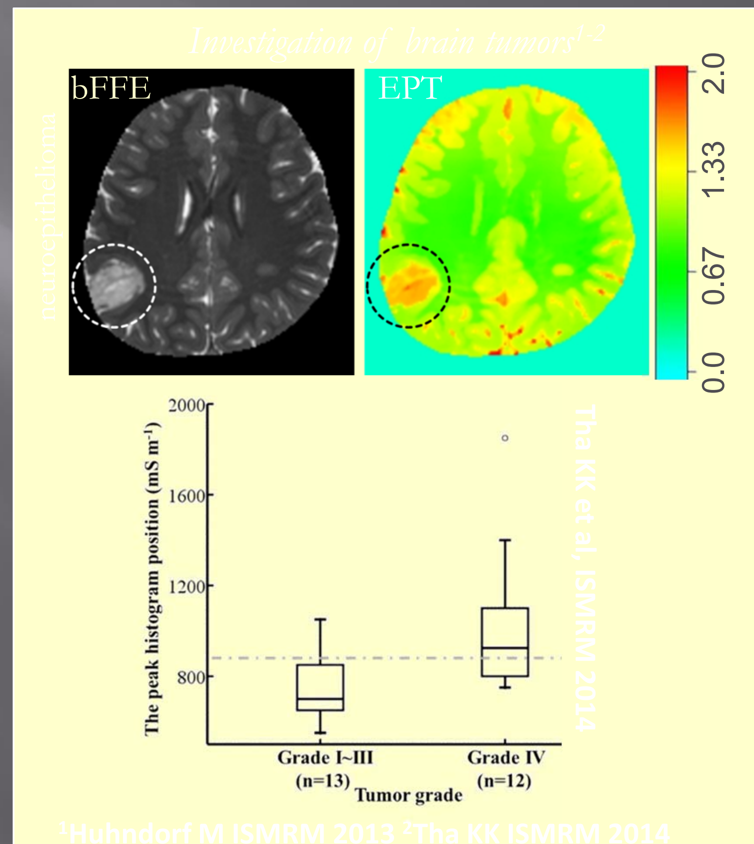

Magnitude, Phase, Conductivity, QSM and T_2*

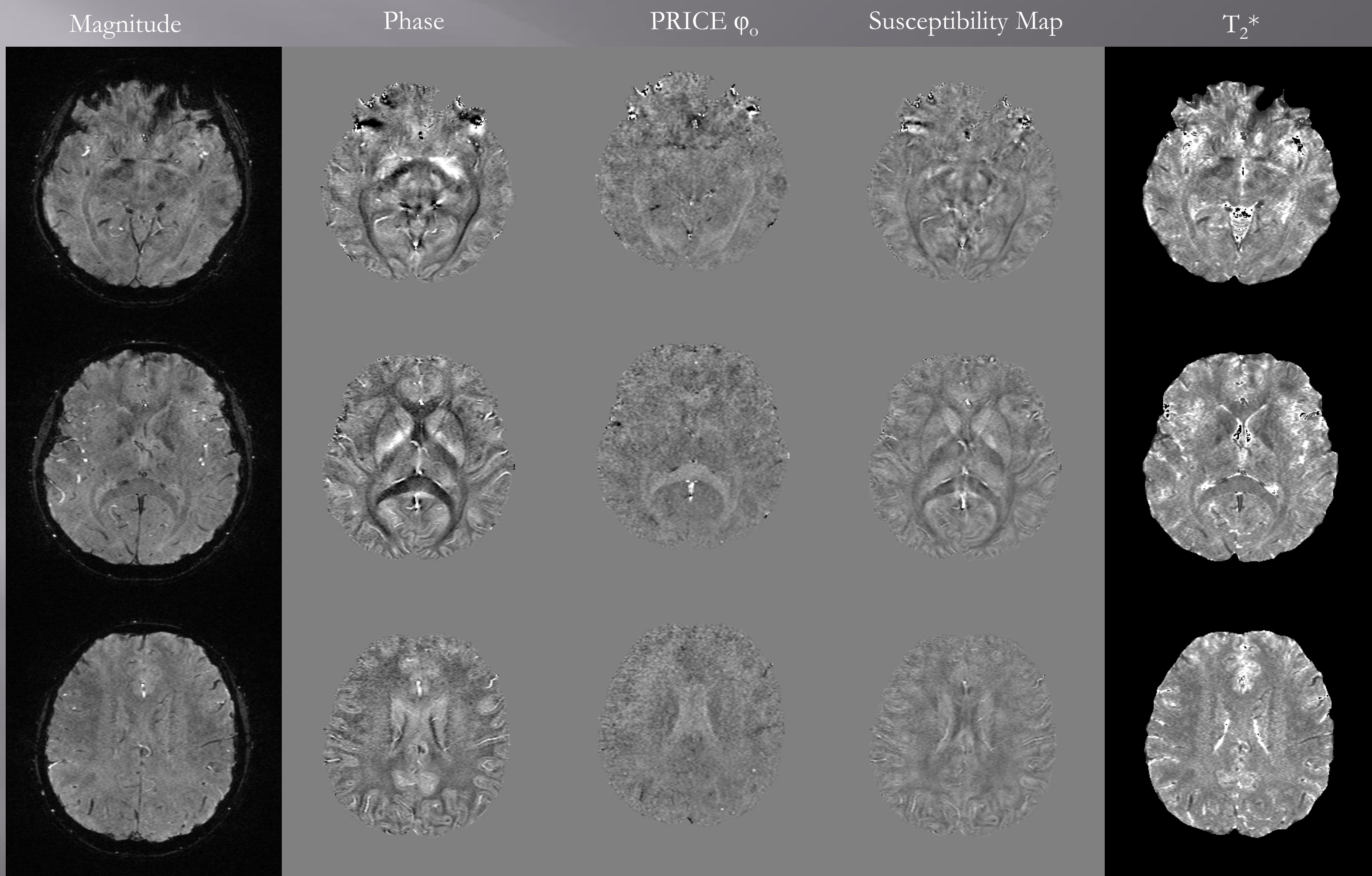

Phase images and PRICE (phase reconstruction induced conductivity enhanced) images were processed using a variable high-pass filter. In additoin, a 2x2 sliding averaging filter was applied to th PRICE images.

Conclusions

- Phase serves as the backbone of imaging concepts in MRI.
- Phase also contains a wealth of information for many different methodologies as demonstrated including some others not discussed today such as elastography and multi-spectral imaging.
- Proper processing of phase is critical to extracting this information.